

Breakdown of a Nocturnal Inversion Measured with a Low-Cost Tethersonde System

A High School Student Experiment

David N. Whiteman, Kofi Boateng, Sara Harbison, Hadijat Oke, Audrey Rappaport, Monique Watson, Ayomiposi Ajayi, Oluwafisayo Okunuga, Ricardo Forno, and Marcos Andrade

ABSTRACT: For the past 4 years, four different cohorts of students from the Science and Technology program at Eleanor Roosevelt High School in Greenbelt, Maryland, have performed their senior research projects at the Howard University Beltsville Research Campus in Beltsville, Maryland. The projects have focused generally on the testing and correction of low-cost sensors and development of instrumentation for use in profiling the lower atmosphere. Specifically, we have developed a low-cost tethersonde system and used it to carry aloft a low-cost instrument that measures particulate matter (PM) as well as a standard radiosonde measuring temperature, pressure, and relative humidity. The low-cost PM sensor was found to provide artificially high values of PM under conditions of elevated relative humidity, likely due to the presence of hygroscopic aerosols. Reference measurements of PM were used to develop a correction technique for the low-cost PM sensor. Profiling measurements of temperature and PM during the breakdown of a nocturnal inversion were performed using the tethersonde system on 30 August 2019. The evolution of temperature during the breakdown of the inversion was studied and compared with model forecasts. The attempt to measure PM during the tethersonde experiment was not successful, we believe, due to the packaging of the low-cost sensor. Future cohorts of students from Eleanor Roosevelt High School students will work on improving the instrumentation and measurements shown here as we continue the collaboration between the Howard University Beltsville Campus and the local school system.

KEYWORDS: Instrumentation/sensors; Radiosonde/rawinsonde observations; Mesoscale models; Education; Aerosol hygroscopicity; Measurements

https://doi.org/10.1175/BAMS-D-21-0150.1

Corresponding author: David N. Whiteman, dnwhiteman@gmail.com, david.whiteman@howard.edu

In final form 14 September 2022 ©2023 American Meteorological Society

For information regarding reuse of this content and general copyright information, consult the AMS Copyright Policy.

AFFILIATIONS: Whiteman—Howard University, Washington, D.C.; Ajayi, Boateng, Harbison, Oke, and Rappaport—University of Maryland, College Park, College Park, Maryland; Watson—Purdue University, West Lafayette, Indiana; Okunuga—Illinois Institute of Technology, Chicago, Illinois; Forno and Andrade—Universidad Mayor de San Andrés, La Paz, Bolivia

Global Atmosphere Watch (GAW 2017) site was established at Mount Chacaltaya (CHC; 5,240 m) in the Bolivian Andes in 2010 (see "Mount Chacaltaya" sidebar). The site is maintained by the Laboratory for Atmospheric Physics (LFA) at the Universidad Mayor de San Andres (UMSA) in La Paz, Bolivia. One of the main motivations for establishing the site was the observed acceleration of the melting of Andean glaciers (Francou et al. 2003; Soruco et al. 2009) and concern over the potential role in this melting of boundary layer–generated aerosols that are transported to higher elevations in the Andes (Wiedensoler et al. 2018; Pérez-Ramírez et al. 2017). A mechanism for the transport of aerosols from lower elevations to higher ones in mountainous regions is the upslope wind created by daytime solar heating (Whiteman 2000; Pal et al. 2017). This phenomenon is also referred to as the mountain chimney effect (MCE) (Lu and Turco 1995). To study this phenomenon in the CHC region, a student-focused experiment was funded by the U.S. State Department through the USA StudyAbroad program (see "Joint Bolivian-U.S. student field measurement campaign" sidebar). The goal was to measure surface winds and the near-surface vertical profile of temperature and particulate matter (PM) fields at several locations along a pollution pathway from the city of La Paz toward the CHC station located approximately 22 km from La Paz. One possible way to measure these vertical profiles is by use of several tethersonde systems working simultaneously along the pollution pathway beginning before sunrise and continuing through the morning during the development of the MCE.

Mount Chacaltaya

Mount Chacaltaya, the location of the Global Atmosphere Watch station that is the focus of the student field experiment mentioned here, was once the location of the world's highest ski resort (Fig. SB1). Skiing took place on the Chacaltaya glacier from the 1930s until 2009 when the glacier fully melted. Earlier predictions indicated that the glacier would last until at least 2015. The accelerated melting of the glacier and the resulting end to the ski resort activities were among the motivators for establishing the GAW site at Mount Chacaltaya.



Fig. SB1. The Global Atmosphere Watch station at Mount Chacaltaya is the world's highest-elevation GAW station at 5.2 km. The peak of Mount Chacaltaya is centered above the station at an elevation of 5.4 km. Photo taken by Marcos Andrade.

Joint Bolivian-U.S. student field measurement campaign

During the period of 21–28 May 2022 seven of the authors here (students Ajayi, Oke, Okunuga, and Watson along with mentors Andrade, Forno, and Whiteman) and others participated in a joint Bolivian-U.S. student field measurement campaign with the U.S. participants being funded by the USA StudyAbroad program of the U.S. Department of State. The field measurements that were performed were in significant measure motivated by the work presented in this manuscript. During the May 2022 experiment, eight Bolivian students and four U.S. students acquired in situ and atmospheric profile measurements at three locations along a canyon leading up to the Chacaltaya GAW station near La Paz in an attempt to quantify the characteristics of the local mountain chimney effect that is believed to be one of the principal mechanisms of pollution transport to the Chacaltaya station (Fig. SB2). Those data are currently being analyzed by all the students working together through weekly virtual sessions.





Fig. SB2. (a) Tethersonde launch preparation at the Curva Uno site on 24 May 2022. From left: Ludving Cano Fernández, Monique Watson, Marco Rivera, Samantha Lobatón, Yahuar Chambi, David Whiteman. Photo taken by Isabel Moreno. (b) From left: Adrian Rodriguez, Alan Callau, and Tania Benadalid setting up the Davis weather station at the Represa site on 24 May 2022. Photo taken by David Whiteman.

We describe here the work done by U.S. high school students in support of the studentfocused experiment held in Bolivia that is described in the "Joint Bolivian-U.S. student field measurement campaign" sidebar. The work described here was performed over a period of 4 years by senior-year students who were involved in the Science and Technology program at Eleanor Roosevelt High School (ERHS) in Greenbelt, Maryland (see "Eleanor Roosevelt High School's Science and Technology program" sidebar). Four separate cohorts were therefore involved in testing the sensors and tethersonde apparatus that could be used in the studentfocused MCE experiment that was held in May 2022. The work was performed at the Howard University Beltsville Campus (HUBC) in Beltsville, Maryland (39.06°N, 76.88°W, 53 m; see "Howard University Beltsville Campus" sidebar), under the mentorship of the first author. It should be noted that all measurements, analyses, and plots presented here were performed

Eleanor Roosevelt High School's Science and Technology program

The Science and Technology program at Eleanor Roosevelt High School in Greenbelt was established in 1976 as the first such magnet program in the Prince George's County Public Schools, a majority African American school district. The program is a rigorous 4-yr course of study that provides intensive academic experiences and college level instruction focused on science, technology, engineering, and mathematics (STEM). Graduates of the program include Sergey Brin, one of the founders of Google. Seven of the coauthors on this manuscript participated in the Science and Tech program and all received generous university scholarship offers, four of which were "full ride."

Howard University Beltsville Campus

The HUBC, where the tethersonde measurements of 30 August 2019 occurred, is a 110 acre mostly wooded facility located in a mixed rural, residential, and business area of Beltsville. It is a campus of Howard University that is devoted to public and private collaborative environmental research and student training primarily through the Howard University Program in Atmospheric Sciences. The campus houses various pieces of atmospheric instrumentation to support student research, has hosted large field measurement campaigns such as NASA's DISCOVER-AQ, hosts an air quality suite owned and maintained by the Maryland Department of the Environment and is the only university member of the GCOS Reference Upper Air Network (GRUAN) within which reference-quality radiosondes are launched at the campus each week.

by the ERHS students. Because the work occurred over a period of 4 years, with different sets of students involved each year, the coordination of the analysis was challenging at times and certain follow-up analyses therefore became more difficult. To preserve continuity of the project, we have generally been fortunate to arrange an overlap of the students during the summer months to "hand off" the project from the students who had just graduated to the rising seniors. This required close coordination with the Science and Technology program, which was quite successful throughout.

The paper is organized as follows. In the first section, we describe earlier low-cost tethersonde efforts that motivated the current work, the details of the tethersonde system that was developed here, and the instrumentation that was used for atmospheric profiling. We also consider the prevailing FAA regulations pertaining to the use of "moored balloons" in the United States. In the second section, we discuss the work done to compare the low-cost PM sensors with those from a federal reference equivalent measurement system. We then describe the tether-sonde profiling experiment that was performed on 30 August 2019, during the presence of a nocturnal temperature inversion, and the analysis of the measurements that were acquired. In the third section, we summarize and conclude the paper and discuss possible future work.

Methods

Related efforts using a home-built tethersonde. In 2018, members of the LFA at UMSA in La Paz built a tethersonde system that uses an electric hand drill, small cart wheel, and high-strength fishing line (Fig. 1). The system was used on 23 June 2018 during the San Juan celebration of the winter solstice when many bonfires are traditionally set on the longest

night of the year. For a period of several hours, ascent and descent measurements of pressure (*P*), temperature (*T*), relative humidity (RH), and black carbon were made with profiles reaching altitudes of 1,000 m AGL. This successful demonstration of the use of a low-cost tethersonde to profile the lower atmosphere motivated the high school student work described here.

Tethersonde apparatus and sensors. To perform similar profiling measurements at HUBC,



Fig. 1. Home-built tethersonde being tested by members of the LFA from the UMSA campus in La Paz on 23 Jun 2018.

a homemade, low-cost tethersonde system was developed that is based on the Bolivian research described above. The tethersonde system has advantages over larger, more costly commercial systems by being capable of performing lower-altitude measurements at greatly reduced cost and, as will be described later, in a manner that is not subject to FAA regulation. The tethersonde was used here to carry aloft a standard iMet-1 radiosonde package manufactured by Intermet Systems as well as a low-cost sensor (LCS) for measuring PM_{2,5} and state variables that was developed at Duke University (Bergin 2021a). The iMet data were recorded in real time on a laptop running NOAA Skysonde software, which received the iMet data using an iCom Rx-7 handheld radio tuned to the 403 MHz signal of the radiosonde. The LCS data were recorded to a micro-SD card on the Teensy Arduino microcontroller and were retrieved after the flight. Figure 2 shows the tethersonde system in use on 30 August 2019 during the experiment to be described later (Fig. 2a), the tethersonde device itself (Fig. 2b), and a close-up of the iMet radiosonde and LCS package partially enclosed in a plastic bag (Fig. 2c). The tethersonde apparatus (Fig. 2b) consists of a variable speed drill with locking trigger coupled to a 12-in.-diameter (\sim 30 cm) blower pulley. High-strength fishing line is guided through a hole in the top plate. The hole in the top plate holds a small-aperture, polished, internally threaded titanium ear tunnel to guide the fishing line on and off the pulley and to reduce friction on the fishing line. This polished titanium ear tunnel was found to be crucial for minimizing friction and reducing problems in alignment of the fishing line and the pulley. The components of the tethersonde system as constructed and used at HUBC on 30 August 2019 and their costs are listed in the appendix.

FAA REGULATIONS. Before conducting operations such as those described here, it is important to consider the prevailing FAA regulations. FAA Regulations Part 101 describes the operational regulations for "moored balloons, kites, amateur rockets, and unmanned free balloons" (FAA 2012). The regulations are applicable to balloons with diameter greater than 6 ft (\sim 1.8 m) or with payloads exceeding 6 lb (\sim 2.7 kg). All operations, regardless of dimensions of the equipment, are required to be conducted in a manner that does not create a hazard to people or property and no objects may be dropped from the balloon. Operations may not occur in restricted or prohibited airspace without permission of the controlling authorities. Provided the device in use does not violate these restrictions, FAA Part 101 does not pertain. One of the attractions of the system described in Table A1 in the appendix is that the balloon size (5 ft; \sim 1.5 m) and package weight (<1 lb; \sim 0.45 kg) are below the limits defined in FAA Part

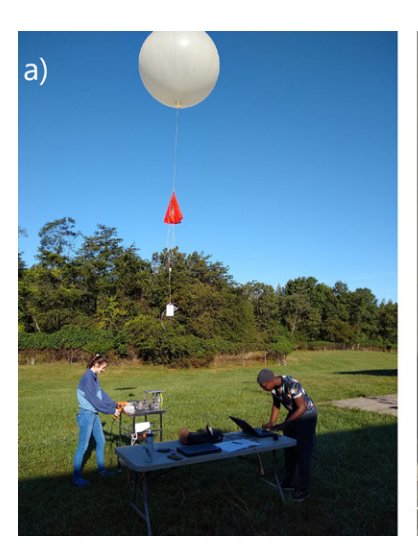






Fig. 2. (a) Early morning on 30 Aug 2019 during the tethersonde experiment with students Sara Harbison and Kofi Boateng. (b) Close-up of the tethersonde device constructed for this experiment. (c) Close-up of the iMet radiosonde with a Duke University LCS device partially enclosed in a plastic bag.

101 while still permitting useful profile measurements to be made. Thus, no coordination with the FAA was required for performing these measurements.

Results

Testing the low-cost sensors. The low-cost sensor that was used for measuring $PM_{2.5}$, RH, and temperature in this research was generously donated by the Bergin group from Duke University (Bergin 2021a). The LCS consists of a Planttower 3003 PM sensor, Sparkfun SHT 15 for measuring T and RH, real-time clock (ChronoDot 2.1), and an Arduino microcontroller (Teensy 3.2) for controlling the sensors and recording the data. Sensors similar to these have been used by the Bergin group to study pollutant levels in underdeveloped areas such as Bolivia (Bergin 2021b) and India (Vreeland et al. 2018).

To characterize the performance of the LCS and to test for possible sensitivity to changing RH conditions (Zheng et al. 2018), two nominally identical LCS units were located and operated alongside of a MetOne BAM 1020 particle sampler, a federal reference equivalent method of measuring $PM_{2.5}$. The BAM 1020 is part of the air quality monitoring station operated by the Maryland Department of the Environment (MDE 2021) and located at HUBC. Measurements of T, P, and RH were also made at the MDE site using a Vaisala WXT536. This Vaisala instrument is changed on an annual basis to maintain the calibration of its measurements. Thus, high-quality RH and $PM_{2.5}$ measurements from the MDE instrumentation were used to characterize the performance of two Duke University LCS systems. Figure 3 displays the measurements of the BAM 1020 and one of the LCS (second sensor provided similar results) from 6 to 28 March 2019.

Some particles such as sulfates and sea salt are known to be hygroscopic and thus can swell in size when the RH exceeds approximately 75%–80% depending on the chemical composition of the aerosol (Martin, 2000; Tang et al. 2019). Such aerosol hygroscopicity has been studied previously based on measurements near HUBC (Veselovskii et al. 2009; Pérez-Ramírez et al. 2021). To normalize measurements of both hygroscopic and nonhygroscopic aerosols, the BAM 1020 dries the PM to approximately 40% RH as part of the measurement process. The Planttower sensors include no such drying feature, and thus, when RH exceeds approximately 75%, differences in the measured PM between the BAM 1020 and the LCS can occur. To study this possibility, the PM_{2.5} measurements in Fig. 3 are shown with the LCS measurements

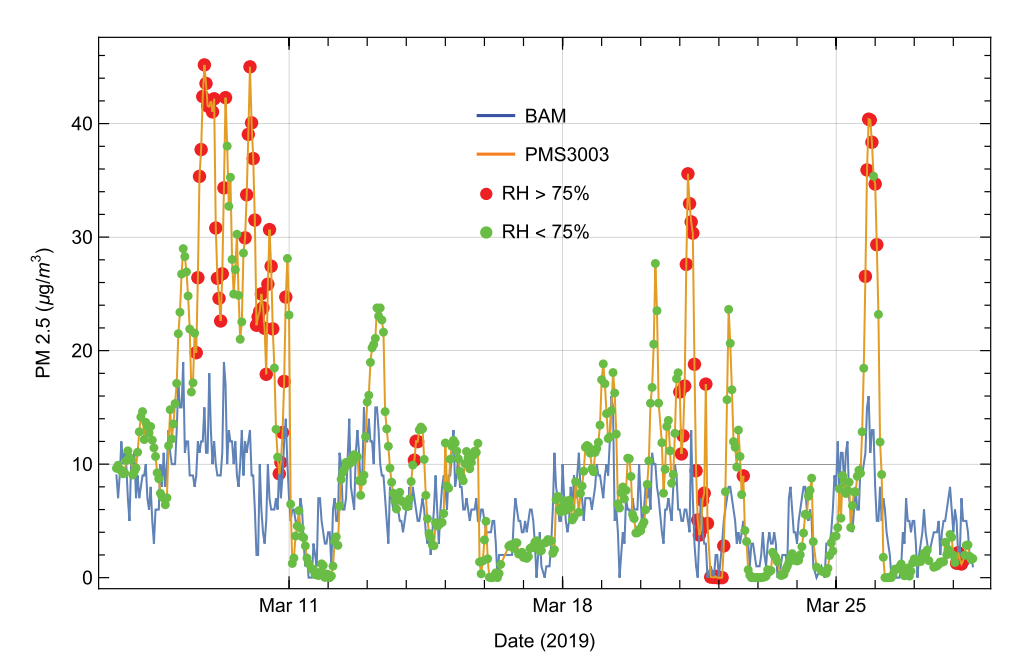


Fig. 3. RH and PM_{2.5} measurements from the BAM 1020 and LCS sensor for the period 6–28 Mar 2019. The LCS PM measurements are separated by RH. See text for details.

being plotted with red dots for ambient RH > 75% and with green dots for RH < 75%, where the RH data from the Vaisala WXT536 were used. Although there are exceptions, in general the peaks in PM_{2.5} concentrations recorded by the PMS3003 sensor occur at times when RH \geq 75%. While the PMS3003 sensor frequently displays peaks in PM_{2.5} concentration at times of high RH, the BAM 1020 sensor does not display a similar correlation between the ambient RH and PM_{2.5} peaks since the BAM 1020 dries the particles as previously stated. We conclude that the peaks of PM_{2.5} concentrations measured by the PMS3003 for RH \geq 75% are likely due to the presence of hygroscopic particles. Figure 3 indicates that the LCS may provide inaccurate measurements in the presence of hygroscopic particles. In the next section we develop and compare three different correction techniques to address this source of uncertainty.

CORRECTION TECHNIQUES FOR ADDRESSING HYGROSCOPIC GROWTH. In an effort to improve the accuracy of the low-cost PM sensor, we present here correction techniques that use the BAM 1020 PM measurements as reference. Three different correction schemes were studied. They are referred to as linear correction (LC), inverse correction (IC), and hygroscopic growth correction (HGC). They all determine a correction of the PMS3003 PM measurements with respect to the BAM 1020, which is considered to be the reference, but use different mathematical approaches for doing so. We will first show the results of applying the three correction techniques and then describe the individual techniques.

For all techniques, the PMS3003 PM $_{2.5}$ measurements were averaged over each hour to align with the BAM 1020 hourly measurements and ordered pairs of hourly BAM and PMS3003 data were formed for the first two techniques and ratios of PMS3003 and BAM 1020 data were formed for the third technique. In the preparation of the data, BAM 1020 PM $_{2.5}$ measurements that were lower than 3 μ g m $^{-3}$ were removed as the BAM 1020 calibration specifications provided by MDE indicate that the calibration holds for PM values exceeding 3 μ g m $^{-3}$. For all three techniques, the data were then split into two sets, the first extending from 6 to 17 March 2019 used for generating the correction equations and the second, from 18 to 28 March 2019, used for testing the three different correction techniques.

Figure 4 presents the original datasets and all three correction approaches for both the training dataset from 6 to 17 March and the test dataset from 18 to 28 March. Table 1 shows

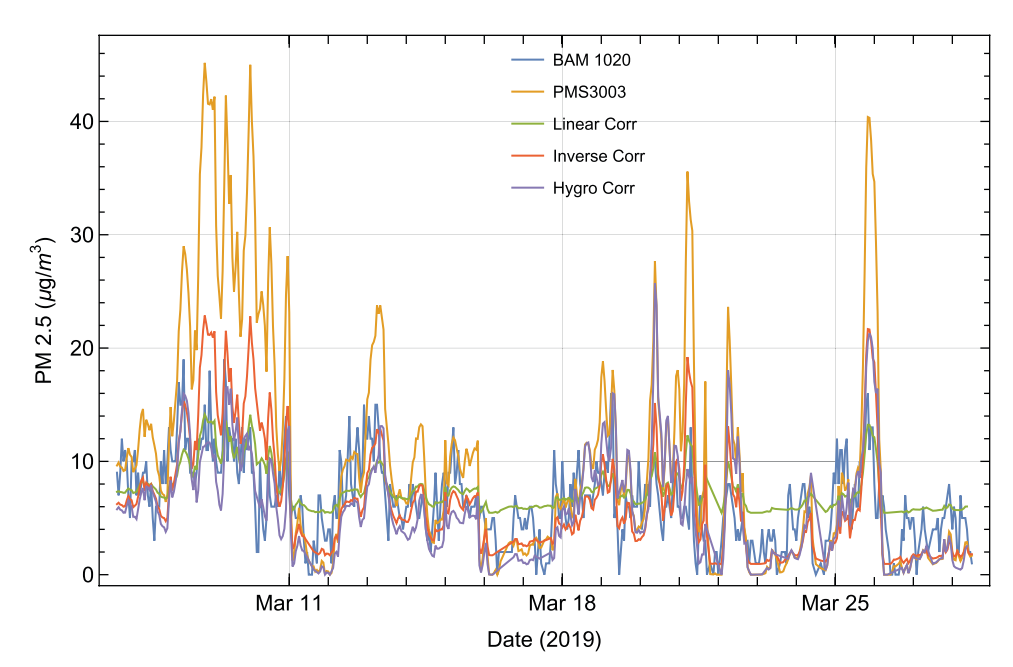


Fig. 4. BAM 1020, PMS3003, linear correction, inverse correction, and hygroscopic growth equation PM_{2.5} measurements collected from 6 to 28 Mar 2019. The period 6–17 Mar data were used to generate the correction equations; 18–28 Mar data were used to test the correction equations.

the root-mean-square error (RMSE) between the BAM 1020 and the corrected LCS data using the three techniques. We will now describe each of the correction techniques explored.

Linear correction. To explore what was called the LC technique, ordered pairs were formed as {PMS3003, BAM} and an unweighted linear regression of these ordered pairs was performed. The reason for using the PMS3003 data as the abscissa coordinate for this regression is that it results in an equation y = f(x),

Table 1. Uncalibrated PMS3003, linear correction, inverse correction, and hygroscopic growth correction RMSE values for the data collected from 6 to 17 Mar 2019 (column 2) and 18 to 28 Mar 2019 (column 3). The measurements from 6 to 17 Mar were used to develop the mathematical forms of the equations. The measurements from 18–28 Mar were used to test the techniques.

Technique	6–17 Mar RMSE (µg m ⁻³)	18–28 Mar RMSE (µg m ⁻³)
Uncalibrated PMS3003	10.8	8.1
Linear correction	3.0	2.5
Inverse correction	4.0	3.6
Hygroscopic growth correction	3.7	4.5

where x is the PMS3003 value and y is the desired corrected PM value. Thus, the equation does not need to be inverted to be applied as will be the case for the next technique considered. The best fit equation of y = 0.19x + 5.5 was determined (Fig. 5a) and then directly applied to the PMS3003 PM_{2.5} measurements to correct the data. A regression of the corrected PMS3003 data versus the BAM 1020 was performed to test the accuracy of the correction and resulted in a best-fit equation with a slope of 1.0 and y intercept of essentially zero (Fig. 5b) indicating that the correction equation is performing as expected. The results in Table 1 indicate that applying the LC technique to the calibration dataset reduced the RMSE from 10.8 to 3.0 and from 8.1 to 2.5 for the test dataset; however, note the compression of the abscissa values to a range of $5-14~\mu g$ m⁻³ in the corrected measurements (Fig. 5b) versus the range prior to correction of 3 to >40 μg m⁻³ that is shown in Fig. 5a. This compression will become important when comparing the three techniques.

Inverse correction. Another method for correcting the LCS data that was explored was called the IC technique. This is a similar technique to the linear correction; however, the BAM data are used as the abscissa coordinate in this case so that the ordered pairs that are regressed are {BAM, LCS}. The best fit linear equation was found to be y = 2.1x - 3.7, as shown in Fig. 6a. The correction equation was created by finding the inverse of this linear equation,

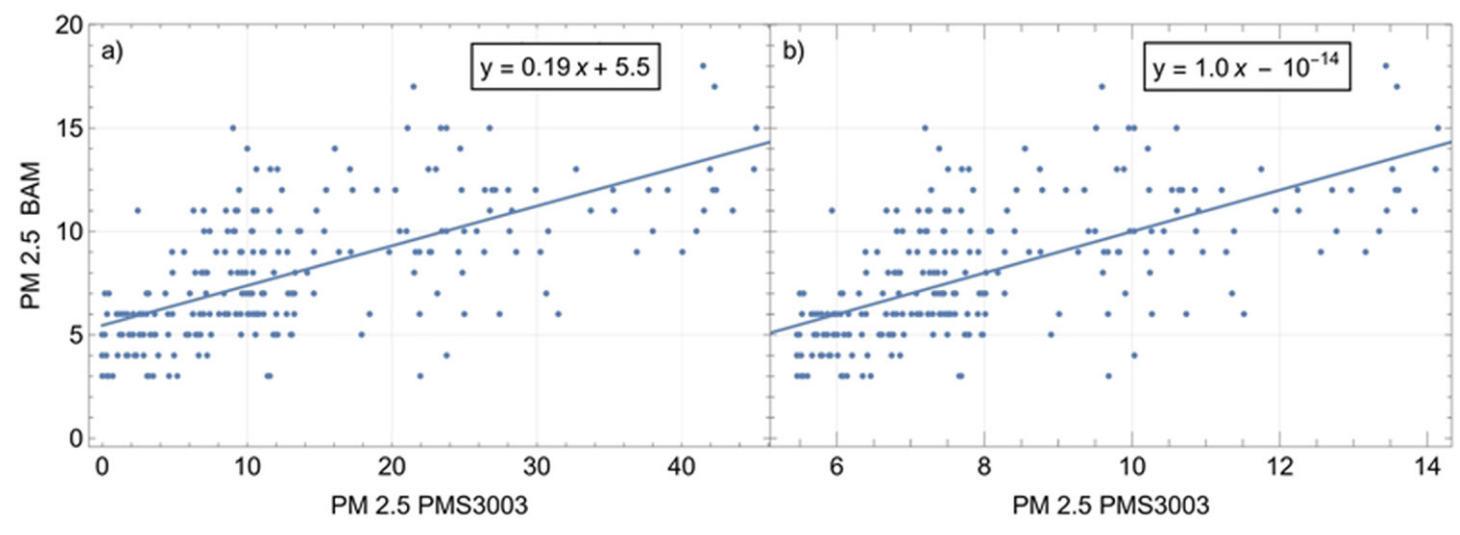


Fig. 5. Linear correction: (a) Linear regression of the reference BAM and original PMS3003 measurements of PM_{2.5} (μ g m⁻³). (b) Linear regression of the same BAM data and the corrected PMS3003.

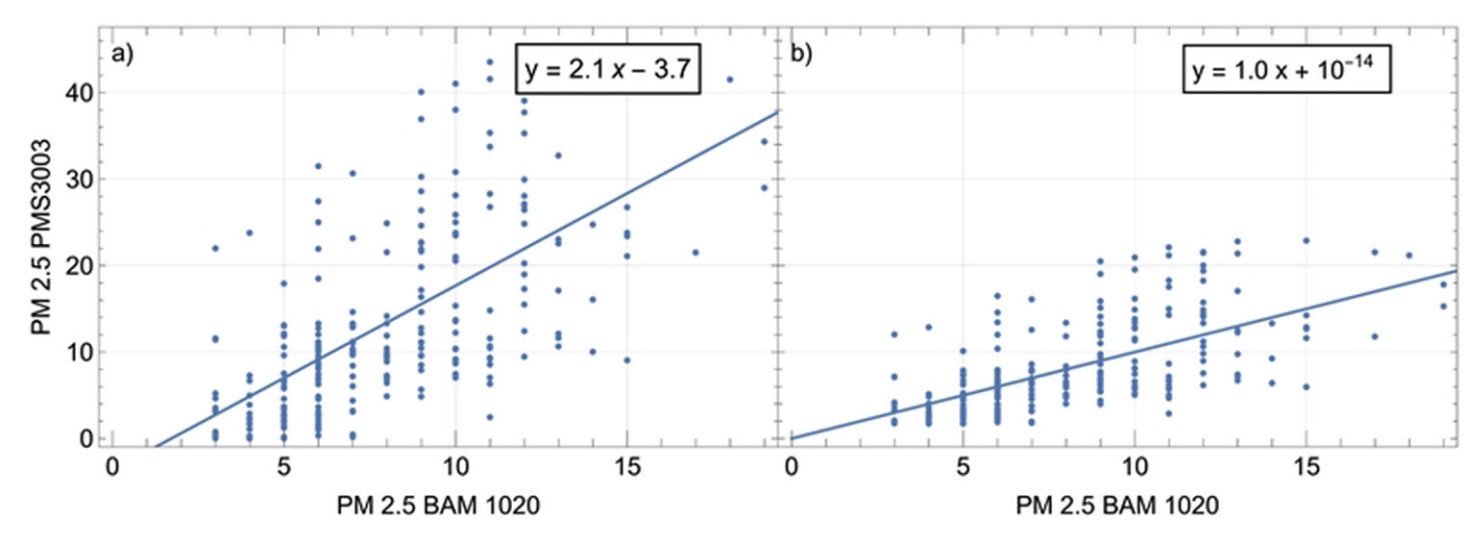


Fig. 6. Inverse correction: (a) Linear regression of BAM 1020 PM_{2.5} measurements and uncorrected PMS3003 PM_{2.5} measurements from 6 to 17 Mar 2019. (b) Linear regression of BAM 1020 PM_{2.5} and calibrated PMS3003 PM_{2.5} measurements.

i.e., y = (x + 3.7)/2.1. As before, the inverse correction was then applied to the same set of data from which it was created to test the equation's accuracy and is shown in Fig. 6b. As expected, the resulting best fit equation had slope of 1.0 with near zero y intercept. The inverse correction reduced the RMSE value from 10.8 to 4 μ g m⁻³ when the correction was applied to the dataset from which it was derived and from 8.1 to 3.6 for the test dataset (Table 1). Careful inspection of Fig. 4, however, indicates that the corrected values using the inverse correction technique did not show the same high-bias tendency in the 11 March and 16–18 March periods as was exhibited by the linear correction technique. By contrast, still considering Fig. 4, the inverse correction results showed a tendency toward high bias with respect to the reference BAM value in the period prior to 11 March.

Hygroscopic growth correction. The final technique explored for correcting the LCS PM data has been used before (Zheng et al. 2018) and was referred to as the hygroscopic growth correction technique. The first step was to find a correction factor ψ through the equation

$$\psi = a + b \left(\frac{\text{RH}^2}{1 - \text{RH}} \right) = \frac{\text{LCS}}{\text{BAM}},$$
 (1)

where a and b are adjustable parameters (Zheng et al. 2018). To determine the correction factor ψ , the LCS measurements were divided by the reference sensor measurements and used in the best fitting procedure with

$$a + b \left(\frac{x^2}{1 - x} \right) \tag{2}$$

being the model equation for the fit. The RH data used were from the MDE measurements, not from the LCS, due to their higher quality. In this study a was found to be 1.03 and b was found to be 0.40, thus making the final equation to calculate the correction factor:

$$\psi = 1.03 + 0.40 \left(\frac{RH^2}{1 - RH} \right). \tag{3}$$

The PMS3003 PM_{2.5} concentrations were then divided by ψ , determined from Eq. (3) above, to create the corrected data. Through this correction method, the RMSE value was lowered from 10.8 to 3.7 for the calibration dataset and from 8.1 to 4.5 for the test dataset, as shown in Table 1. Figure 7 displays ψ versus RH and shows that as RH increases above approximately 75%, ψ increases rapidly.

Selection and testing of the preferred correction technique. The three candidate corrections were then compared to choose the preferred technique to use in processing the data acquired during the tethersonde experiment. The linear correction made the greatest improvement in the RMSE values, but, as previously mentioned, it did so by compressing both the high and low extremes in the corrected values. This compression can be observed in Fig. 5b where the range of the abscissa values is approximately 5–14 and where, during the periods of 11 March and 16–18 March in Fig. 4, the corrected PMS data show an artificially high bias. This compression effect is related to using the less accurate PM values from the PMS3003 as the abscissa in the linear regression, which created a non-single-valued relationship between the reference BAM and PMS3003 data. For this reason, despite having the lowest RMSE, we rejected the LC as the preferred correction technique.

The IC and HGC correction techniques produced similar RMSE values for both the datasets; however, visual inspection of Fig. 4 seems to indicate a generally low bias in the HGC corrected values when compared with the reference. Application of the HGC technique also requires that RH be measured accurately in the environment of the PMS3003 sensor, which was not the case during the tethersonde experiment as will be described later; therefore, the HGC technique could not be chosen as the preferred correction method for the tethersonde measurements. Since the inverse correction provided a similar RMSE value to the other methods, did not create what appears to be an artificially high bias during low-PM conditions, and did not require knowledge of the RH, the inverse correction technique was selected for processing the PMS3003 data acquired during the tethersonde experiment.

TETHERSONDE EXPERIMENT OF 30 AUGUST 2019. On clear nights, radiational cooling at Earth's surface can create a shallow region of the atmosphere where temperatures are found to

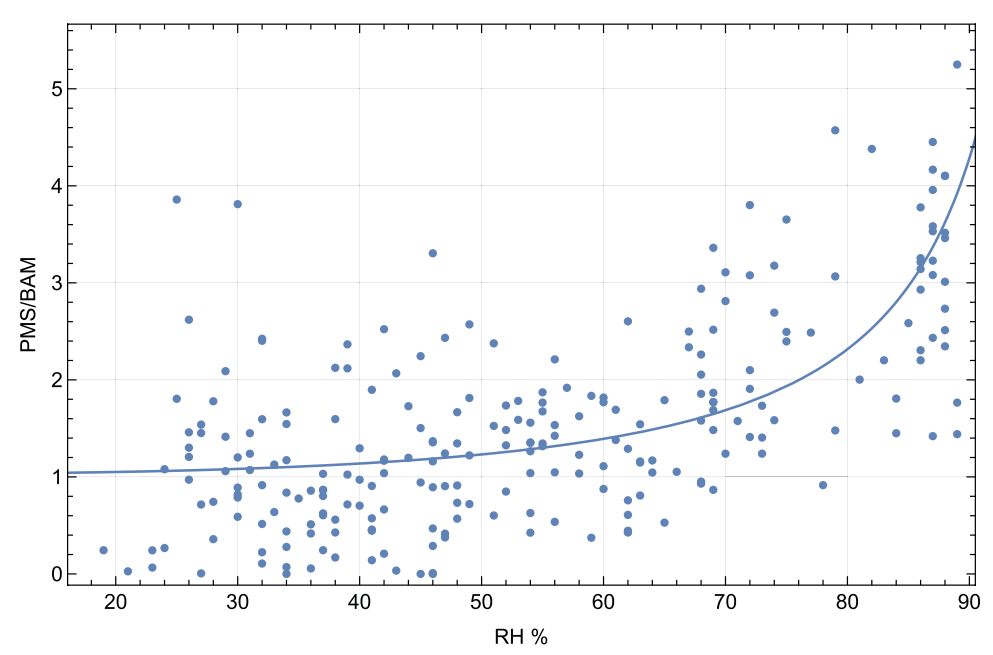


Fig. 7. Hygroscopic growth correction factor ψ plotted vs RH using PM_{2.5} measurements collected from 6 to 17 Mar 2019.

increase with height, instead of the more usual decrease with height, creating what is known as a nocturnal inversion. The night of 29 August 2019 was forecast to be clear, thus setting up the conditions for the development of such an inversion. Just prior to sunrise on 30 August 2019 tethersonde ascents and descents began and continued for 3 h at HUBC in Beltsville. Each ascent–descent pair required approximately 10-15 min to perform and ascent rates of 1-3 m s⁻¹ were used. The 150 g balloon was inflated to a diameter of approximately 5 ft (~ 1.5 m) and was used to carry aloft an instrument complement that consisted of an Intermet iMet-1 radiosonde and a Duke University LCS, which was removed from its housing and placed inside a partially closed plastic bag for protection of the electronics from the elements as shown in Fig 2c.

To illustrate the potential for the tethersonde measurements to be used in model validation, Fig. 8 shows comparisons of temperature measurements from 30 August with forecast data from the NOAA High-Resolution Rapid Refresh (HRRR) model (Dowell et al. 2022; James et al. 2022). Only a single set of comparisons is shown; therefore, these results should not be taken to indicate any general behavior of the HRRR model but instead this comparison illustrates the potential to develop a statistical set of comparisons for model validation purposes. The HRRR model data shown in Fig. 8 have 3 km spatial resolution and 1 h temporal resolution; therefore, the measured temperature profile most closely matching the HRRR forecast time was chosen for the comparisons shown. The figure shows four separate panels for the comparisons of HRRR forecast and tethersonde measurements at 1100, 1200, 1300, and 1400 UTC.

Focusing first on the radiosonde temperature measurements, we note that some deviations in the altitudes and measured temperatures can be noted such as at the top of the first profile and elsewhere in the figure. These are assumed to be due to uneven ventilation of the radiosonde caused by the swinging of the package as it hung below the balloon. The first two profiles (1100 and 1200 UTC) show the largest difference in temperature from lowest to highest altitudes. They both follow a similar pattern of increasing temperature from the surface located at 53 m MSL to an altitude of approximately 160 m MSL indicating the presence of the temperature inversion. Above \sim 150–160 m MSL, the temperature decreases in the first two profiles. By the time of the third profile at 1300 UTC, the temperature inversion had mostly broken down, and by the fourth profile at 1400 UTC a more typical decrease in temperature with altitude was observed with the total change in temperature along the profile of approximately 2°C in rough agreement with an adiabatic lapse rate. We speculate

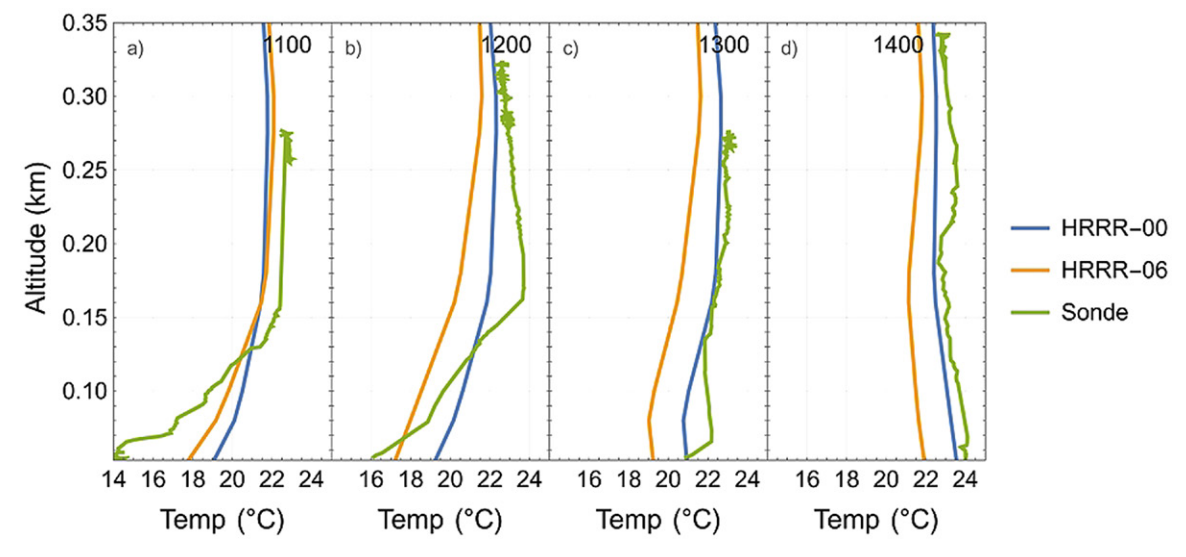


Fig. 8. Comparison of radiosonde measured temperature and forecasts from the HRRR model over at (a) 1100, (b) 1200, (c) 1300, and (d) 1400 UTC. Two initializations of the model at 0000 and 0600 UTC were studied.

that solar heating of the surface led to mixing of the air in the lower atmosphere helping to both break down the inversion as well as create a more usual temperature decrease with altitude.

Two HRRR model forecasts were compared with the tethersonde temperatures: one initialized at 0000 UTC 30 August (approximately 11 h before measurements were started: shown in blue) and the other initialized at 0600 UTC 30 August (approximately 5 h before; shown in orange) and are shown in Fig. 8. We note that neither HRRR forecast accurately forecast the magnitude of the temperature inversion measured at the HUBC site. Measurements indicated an inversion temperature difference between the surface and ~160 m MSL of approximately 8°C while both model runs indicated a difference of ap-

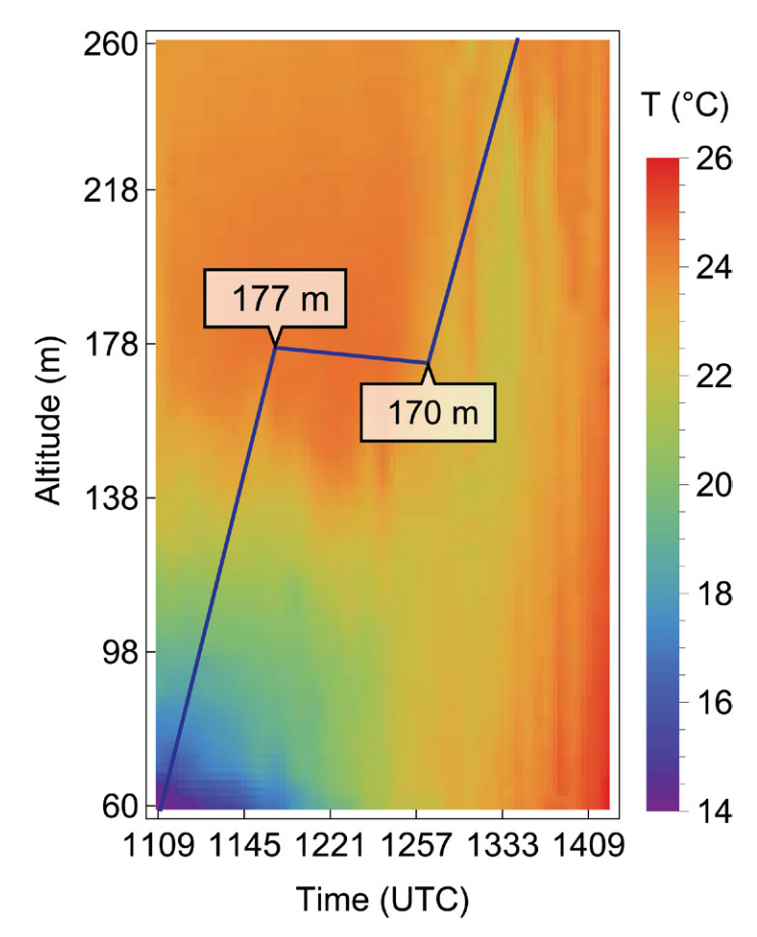


Fig. 9. Interpolated color map of iMet radiosonde temperature measurements on 30 Aug 2019 with PBL heights (dark blue line and inset values) from the HRRR model. Altitude is meters above mean sea level. Surface elevation is 53 m MSL.

proximately 5°C. Furthermore, the temperature inversion appears to have persisted longer in the measurements than in the model predictions with the inversion still evident near the surface at 1300 UTC in the measurements but not in the forecasts. We finally note that the comparisons from the latter 2 h shown in Fig. 8 indicate a generally cold bias of the model with respect to the measurements.

To better visualize the time-height evolution of temperature during the experiment, the radiosonde temperatures were interpolated both as a function of altitude and time to create a regular array of values that could be displayed as a color map as shown in Fig. 9. After sunrise, direct radiation by the sun creates thermals that cause mixing of air masses and influence the evolution of the temperature structure. Near sunrise at 1100 UTC, a cold pool was observed close to the surface and extended upward approximately 100 m until approximately 1221 UTC after which time the temperature below ~130 m became more constant and then decreased with altitude as mentioned with respect to Fig. 8. The PBL height from the HRRR model forecast is also shown in the figure indicating that at the beginning of the measurement sequence, the PBLH was essentially at the surface. As time progressed and the surface was heated, the cold pool dissipated and the forecast PBLH increased to approximately 170 m within the first 2 h of measurements and then to over 300 m by 1400 UTC.

Investigation of PM measurements acquired during the tethersonde experiment. As mentioned earlier, a Duke University LCS device was part of the instrumentation package used during the tethersonde experiment of 30 August 2019. Figure 10 depicts the PM

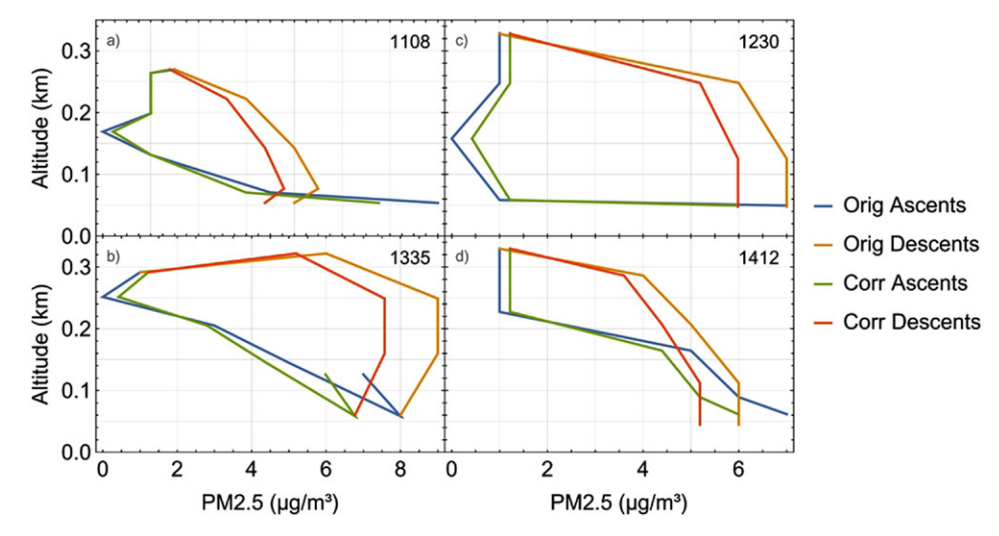


Fig. 10. $PM_{2.5}$ concentration vs altitude data split between ascents and descents using both uncorrected and corrected data.

concentrations measured during adjacent ascents and descents at different times. Both the original and corrected PM data are presented where the inverse correction technique was used for processing the measurements. With the ascents and descents being separated by approximately 10 min in time, one would expect that adjacent profiles would display similar PM values with altitude. What is seen in Fig. 10 instead are loops indicating the presence of significant hysteresis in the measurements whether considering the raw or corrected PM values. The inconsistent measurements shown in Fig. 10 are likely a result of how the LCS sensor was packaged for the tethersonde experiment. To protect the electronics from moisture, as mentioned earlier and shown in Fig. 2c, the LCS device was placed in a plastic bag with openings for the PM sensor inlet and for ventilation. From the appearance of Fig. 10, however, we conclude that the ventilation was insufficient and that the environment inside the plastic bag did not reflect the ambient environment thus resulting in the hysteresis effect shown in the figure. The PM data from the tethersonde experiment were not studied further due to this problem.

Summary, conclusions, and future work

We have presented work performed by high school seniors involved in the Science and Technology Program at Eleanor Roosevelt High School in Greenbelt during the school years of 2018/19, 2019/20, 2020/21, and 2021/22. The work has focused on the characterization and use of low-cost PM sensors, standard radiosondes and a home-built tethersonde system to profile the lower 250 m of the atmosphere during the breakdown of a nocturnal temperature inversion.

Our work in low-cost sensors has indicated that, with correction, inexpensive PM sensors can be useful for charting change in PM concentrations although the difficulty of correcting for possible hygroscopic growth increases the likelihood of errors in absolute concentration measurements of the LCS PM measurements. Nonetheless, the LCS PM sensors we tested are generally robust at detecting changes in PM. To take advantage of this, we envision deploying a small network of PM sensors to study the flow of PM across the network. As a part of this future work, we are developing our own version of the LCS using updated components for measuring PM, *T*, RH, and atmospheric pressure.

We are also encouraged by the initial exploratory comparison of tethersonde temperature measurements and HRRR model forecasts. Future work will be done to create a larger ensemble of such comparisons for a statistical study of model intercomparisons. We also plan to create a well-ventilated package to house the LCS instrument for use in future tethersonde experiments to address the hysteresis observed in the experiment performed here.

The activities described here have provided excellent research experiences for high school seniors. These experiences have broadened their exposure to atmospheric science and instrumentation as they decide their future career paths. We look forward to continuing these efforts through a close coordination with Eleanor Roosevelt High School.

Acknowledgments. We wish to gratefully acknowledge Ryan Auvil, Adam Reese, Joel Dreessen, James Boyle, and David Krask of the Maryland Department of the Environment for their continuous and expert support of various student-focused activities at the HU Beltsville campus including this research effort focused on low-cost sensors. Dr. Michael Bergin and his group at Duke University graciously provided multiple sensor packages that were tested during this research and that now serve as models for future development. We very much appreciate the efforts of Dr. David Turner of NOAA ESRL, Boulder, Colorado, who provided the HRRR model simulations for the tethersonde experiment and who has been generous with his time in entertaining follow-up questions. We also thank Y. J. Twu, coordinator of the ERHS Science and Technology internship program, for her excellent coordination and support of these research efforts. The work described here was done on a voluntary basis by the main author. We gratefully acknowledge the support of the U.S. State Department through the USA StudyAbroad program for support of the student field campaign mentioned in the "Joint Bolivian—U.S. student field measurement campaign" sidebar.

Data availability statement. A Mathematica notebook and associated data files that permit generating all the plots shown in this manuscript are available upon request to the corresponding author.

Appendix: Components of the tethersonde system

The tethersonde system was based on a variable-speed hand drill, large-diameter pulley, and high-strength fishing line. The various components used in the system and their approximate costs are listed in Table A1.

Table A1. Components and approximate costs of the items comprising the tethersonde and measurement system used at HUBC for conducting the profiling measurements on 30 Aug 2019. Note that 1 in. = 2.54 cm.

Component	Approximate cost
VonHaus 10 A variable-speed drill with speed adjustment and lock	\$55
Lasco 05-1184 blower pulley 3/4 in. shaft	\$25
KastKing SuperPower braided fishing line, 1,000 m	\$40
PillowBlock bearings	\$20
Seville Classics kitchen cart	\$100
Stainless steel rod, $3/4$ in. \times 12 in.	\$20
Machining costs to turn rod down from 3/4 in. to 1/2 in.	\$100
Intermet iMet-1 RSB research radiosonde	\$240
iCom Rx-7	\$200
Skysonde software (free download from NOAA)	\$0
Laptop	\$150
Duke University LCS PM T, RH sensor. The particle matter sensors were developed at Duke University and donated to the project. Cost of parts for the LCS is approximate.	\$50
150 g latex meteorological balloon	\$20
Parachute	\$10
Helium	\$50
Total	~\$1,080

References

- Bergin, M., 2021a: Welcome to the Bergin group. Duke University, accessed 8 May 2021, https://bergin.pratt.duke.edu/.
- —, 2021b: An undergraduate hands-on research experience in Bolivia. Duke University, accessed 8 May 2021, https://bergin.pratt.duke.edu/news/undergraduate-hands-research-experience-bolivia.
- Dowell, D. C., and Coauthors, 2022: The High-Resolution Rapid Refresh (HRRR): An hourly updating convection-allowing forecast model. Part I: Motivation and system description. *Wea. Forecasting*, **37**, 1371–1395, https://doi.org/10.1175/WAF-D-21-0151.1.
- FAA, 2012: Part 101: Moored balloons, kites, amateur rockets and unmanned free balloons. FAA Doc., 6 pp., www.govinfo.gov/content/pkg/CFR-2012-title14-vol2/pdf/CFR-2012-title14-vol2-part101.pdf.
- Francou, B., M. Vuille, P. Wagnon, J. Mendoza, and J.-E. Sicart, 2003: Tropical climate change recorded by a glacier in the central Andes during the last decades of the twentieth century: Chacaltaya, Bolivia, 16°S. *J. Geophys. Res.*, **108**, 4154, https://doi.org/10.1029/2002JD002959.
- GAW, 2017: WMO Global Atmosphere Watch (GAW) implementation plan: 2016-2023. GAW Rep. 228, 84 pp.
- James, E. P., and Coauthors, 2022: The High-Resolution Rapid Refresh (HRRR): An hourly updating convection-allowing forecast model. Part II: Forecast performance. Wea. Forecasting, 37, 1397–1417, https://doi.org/10.1175/ WAF-D-21-0130.1.
- Lu, R., and R. P. Turco, 1995: Air pollutant transport in a coastal environment—II: Three-dimensional simulations over Los Angeles basin. *Atmos. Environ.*, **29**, 1499–1518, https://doi.org/10.1016/1352-2310(95)00015-Q.
- Martin, S. T., 2000: Phase transitions of aqueous atmospheric particles. *Chem. Rev.*, **100**, 3403–3454, https://doi.org/10.1021/cr990034t.
- MDE, 2021: Maryland Department of the Environment. Maryland.gov, accessed 8 May 2021, https://mde.maryland.gov/Pages/index.aspx.
- Pal, S., T. R. Lee, and S. F. J. De Wekker, 2017: A study of the combined impact of boundary layer height and near surface meteorology on the CO diurnal cycle at a low mountaintop site using simultaneous lidar and in-situ observations. *Atmos. Environ.*, 164, 165–179, https://doi.org/10.1016/ j.atmosenv.2017.05.041.

- Pérez-Ramírez, D., and Coauthors, 2017: Multi year aerosol characterization in the tropical Andes and in adjacent Amazonia using AERONET measurements. *Atmos. Environ.*, 166, 412–432, https://doi.org/10.1016/j.atmosenv.2017.07.037.
- —, D. N. Whiteman, I. Veselovskii, R. Ferrare, G. Titos, M. J. Granados-Muñoz, G. Sánchez-Hernández, and F. Navas-Guzmán, 2021: Spatiotemporal changes in aerosol properties by hygroscopic growth and impacts on radiative forcing and heating rates during DISCOVER-AQ 2011. Atmos. Chem. Phys., 21, 12 021–12 048, https://doi.org/10.5194/acp-21-12021-2021
- Soruco, A., C. Vincent, B. Francou, and J. F. Gonzalez, 2009: Glacier decline between 1963 and 2006 in the Cordillera Real, Bolivia. Geophys. Res. Lett., 36, L03502, https://doi.org/10.1029/2008GL036238.
- Tang, M., and Coauthors, 2019: A review of experimental techniques for aerosol hygroscopicity studies. Atmos. Chem. Phys., 19, 12631–12686, https:// doi.org/10.5194/acp-19-12631-2019.
- Veselovskii, I., D. N. Whiteman, A. Kolgotin, E. Andrews, and M. Korenskii, 2009: Demonstration of aerosol property profiling by multiwavelength lidar under varying relative humidity conditions. *J. Atmos. Oceanic Technol.*, 26, 1543–1557, https://doi.org/10.1175/2009JTECHA1254.1.
- Vreeland, H., and Coauthors, 2018: Collaborative efforts to investigate emissions from residential and municipal trash burning in India. RTI Press Res. Brief, 8 pp., https://doi.org/10.3768/rtipress.2018.rb.0019.1809.
- Whiteman, C. D., 2000: *Mountain Meteorology*. Oxford University Press, 355 pp.
- Wiedensohler, A., and Coauthors, 2018: Black carbon emission and transport mechanisms to the free troposphere at the La Paz/El Alto (Bolivia) metropolitan area based on the Day of Census (2012). *Atmos. Environ.*, **194**, 158–169, https://doi.org/10.1016/j.atmosenv.2018.09.032.
- Zheng, T., M. H. Bergin, K. K. Johnson, S. N. Tripathi, S. Shirodkar, M. S. Landis, R. Sutaria, and D. E. Carlson, 2018: Field evaluation of low-cost particulate matter sensors in high- and low-concentration environments. *Atmos. Meas. Tech.*, 11, 4823–4846, https://doi.org/10.5194/amt-11-4823-2018.